วิศวกรรมสารฉบับวิจัยและพัฒนา
Engineering Journal of Research and Development
วิศวกรรมสถานแห่งประเทศไทย ในพระบรมราชูปถัมภ์
The Engineering Institute of Thailand under H.M. The King's Patronage

ปีที่ 29 ฉบับที่ 2 เมษายน-มิถุนายน 2561
Volume 29 Issue 2 April-June 2018

Received 13 November 2017
Revised 28 December 2017
Accepted 9 January 2018

ESTIMATION OF SALT-SOLUTIONED CAVERN GEOMETRY FROM SUBSIDENCE TROUGH CONFIGURATIONS UNDER SUPER-CRITICAL CONDITION

Naruemol Saoanunt[1], Supattra Khamrat[2], Thanittha Thongprapha[2] and Kittitep Fuenkajorn[3]

[1]Graduate Student, Geomechanics Research Unit, Suranaree University of Technology, Thailand

[2]Resercher, Geomechanics Research Unit, Suranaree University of Technology, Thailand

[3]Professor, Geomechanics Research Unit, Suranaree University of Technology, Thailand

บทคัดย่อ

งานวิจัยนี้ได้ดำเนินการทดสอบด้วยแบบจำลองทางกายภาพเพื่อศึกษาการทรุดตัวของผิวดินที่มีผลกระทบของขนาดและรูปร่างของโพรงเกลือที่เกิดจากการละลายบริเวณรอยต่อระหว่างชั้นเกลือหินและชั้นดินปิดทับด้านบน ทรายละเอียดขนาด 2 มิลลิเมตร ได้นำมาใช้เพื่อจำลองชั้นดินปิดทับ การทรุดตัวสูงสุดและความกว้างของการทรุดตัวถูกวัดด้วยเลเซอร์สแกนเนอร์ใน 3 มิติ และได้ทำการจำลองโดยใช้ระเบียบวิธีเชิงตัวเลขด้วยโปรแกรม PFC เพื่อนำผลมาเปรียบเทียบกับผลการจำลองทางกายภาพ และสร้างความสัมพันธ์กับรูปร่างของโพรงเกลือภายใต้ความเค้นยึดติดและมุมเสียดทานของชั้นดินปิดทับในระดับต่างกัน ผลงานวิจัยระบุว่าความลึกและความกว้างของการทรุดตัวของผิวดินมีค่าเพิ่มขึ้นเมื่อโพรงละลายเกลือมีความกว้างและความสูงมากขึ้น ภายใต้ความสูงของโพรงที่เท่ากัน การทรุดตัวสูงสุดมีค่าลดลงเพียงเล็กน้อยเมื่อชั้นหินปิดทับมีความหนามากขึ้น ผลจากการจำลองทางคอมพิวเตอร์มีความสอดคล้องกับผลที่ได้จากแบบจำลองทางกายภาพเป็นอย่างดี ชุดของสมการเชิงประจักษ์ถูกพัฒนาขึ้นเพื่ออธิบายผลการทดสอบและผลที่ได้จากการจำลองด้วยคอมพิวเตอร์ ซึ่งสมการดังกล่าวสามารถนำมาใช้ประเมินความสูงและความกว้างของโพรงละลายเกลือโดยใช้ข้อมูลจากรูปทรงของการทรุดตัวบนผิวดินและคุณสมบัติเชิงกลศาสตร์ของชั้นหินปิดทับ

ABSTRACT

Physical model tests are performed using a trap door apparatus to simulate surface subsidence as affected by size and shape of salt-solution caverns created at the interface between salt and overlying soil formations. Fine sand (2 mm) is used as overburden material. The maximum subsidence and trough width are measured using 3-D laser scanner. Numerical simulations using PFC code are performed to compare with the model results and to correlate the cavern geometries under a variety of cohesions and friction angles of the overburden. The results indicate that the surface subsidence and trough width increase with increasing cavern width and height. Under the same cavern height, the maximum subsidence slightly decreases with increasing the overburden thickness. The computer model results agree well with those obtained from the physical model results. Set of empirical equations is derived to fit with the physical model results, which can be used to estimate the cavern height and width from the subsidence trough configurations and overburden mechanical properties.

KEYWORDS: Subsidence, Cavern, Salt, Physical Model

1. Introduction

Salt and associated minerals in the Khorat and Sakon Nakhon basins, northeast of Thailand have become important resources for mineral exploitation and for use as host rock for product storage. For over five decades, local people have extracted the salt near ground surface by using an old-fashioned technique, called here the 'brine pumping' method. A shallow borehole is drilled into the rock unit directly above the salt. Brine (saline groundwater) is pumped through the borehole and left to evaporate on the ground surface. This simple and low-cost method can, however, cause an environmental impact in the form of unpredictable ground subsidence, sinkholes, and surface contamination [1]. The subsidence or sinkhole is caused by deformation or collapse of the cavern roof at the interface between the salt and overburden. This usually occurs during dry season where the cavities loss the support from the groundwater. Exploratory drilling and geophysical methods (e.g., resistivity and seismic surveys) have normally been employed to determine the size, depth, and location of the underground cavities in the problem areas in an attempt to backfill the underground voids, and hence minimize the damage to the engineering structures and farmland on the surface [2-4]. The geophysical and drilling investigations for such a widespread area are costly and time-consuming. This calls for a quick and low-cost method to determine the size, and shape of the solution caverns. The method may be used as an early warning tool so that mitigation can be implemented before the uncontrollable and severe subsiding of the ground surface occurs.

Numerical methods have also been widely employed for the subsidence analysis, primarily to predict the maximum subsidence, and size and shape of the subsidence trough. The extent of subsidence area is predominantly controlled by geological conditions of the overburden strata. A variety of numerical codes have been used ranging from non-linear, linearly elastic, plastic, to visco-elastic plastic models [5-9]. The main drawback of the numerical approaches is that they require representative material parameters and accurate boundary and loading conditions of the simulated domains. This means that extensive laboratory and field testing and measurements are required to obtain the representative input parameters.

Physical modelling has long been a research tool for understanding of the subsidence mechanisms [10-12]. Several modeling techniques has been developed worldwide to study the ground responses to the underground excavations. These techniques range from two-dimensional trap door tests to miniature tunnel boring machines that can simulate the process of tunnel excavation and lining installation in a centrifuge [13-14]. The primary advantage of the physical or scaled-down model test is that the boundaries and material properties can be well controlled, and hence provides the results that are isolated from the effects of material inhomogeneity and the complex shape of the underground caverns.

This study is focused on the estimation of the solutioned cavern height and width at the interface between salt bed and overlying soil formation. Series of physical model simulations and numerical analyses are performed under a variety of cavern sizes, shapes and depths. Mathematical relationships are proposed to link the cavern geometries with the subsidence trough configurations and overburden properties.

2. Testing Material and Apparatus

Fine sand with nominal sizes of 2 mm is used as the test material. Efforts are made to determine the grain size distribution and shearing resistance. The grain size analysis and calculation follow the ASTM D422-63 [15] standard practice. The uniformity coefficient (Cu) is 1.29 and the coefficient of curvature (Cc) is 1.07. The sand is classified as poorly graded in accordance with ASTM D2487-06 [16]. Based on Power [17] classification system, the sphericity of the sand is high and the roundness is subangular. The direct shear test is performed to determine the cohesion and friction angle of the sand using ASTM D5607-08 [18] standard practice. Based on the Colomb criterion the cohesion of material is 15.61 kPa, and friction angle is 22.7 degrees. The normal and shear stiffness of the sand are 44.54 and 0.73 GPa/m.

A trap door apparatus [19] is used in the physical model simulations, as shown in Figure 1(a). For each test series, the sample container is filled with the sand to a pre-defined thickness which represents thickness of overburden. The sand is lightly packed and the top surface is flattened before starting the test. The underground opening is simulated by carefully pulling down the plastic blocks underneath the sample container. The opening is created at the center of the sand container to ensure that the induced subsidence is clear from the container edges.

The opening width (W) is varied from 10 mm to 50 mm. The opening length (L) is 200 mm. The opening height (H) is varied from 25, 50, 75 to 100 mm. The overburden thickness or opening depth (Z) is from 100 to 300 mm with 50 mm interval. Figure 1(b) shows the test parameters and variables defined in the simulations. After the underground opening is created, the settlement of the top surface occurs. The laser scanner measures the surface profile of the sand before and after the subsidence is induced. The measurements are made to the nearest 0.01 mm. An example of a scanned image is shown in Figure 2. Each opening configuration is simulated at least 3 times to verify the repeatability of the results.

3. Test Results

The measurement results are presented in terms of the maximum subsidence (S_{max}) and trough width (B). Examples of the maximum subsidence measurements (S_{max}) as a function of the opening height (H) for each opening width (W) are shown in Figure 3(a). The trough widths (B) as a function of opening width are given in Figure 3(b). The results indicate clearly that the maximum subsidence and trough width increases with increasing opening height and opening width. This is simply because under super-critical conditions, the material can collapse (flow) into the opening more easily, and hence induces larger trough width. The maximum subsidence tends to decrease as the overburden thickness (Z) increases due to the inter-locking of the particles above the opening [15,20]. Note that the S_{max} values are more sensitive to the opening height for the wide openings than for the narrow ones (Figure 3(a)). More discussions on the test results are given in the following sections.

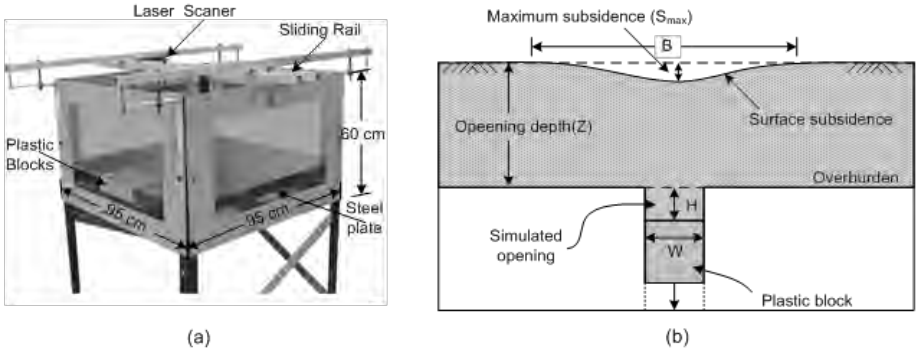

Figure 1 Trap door apparatus [19] (a), and the variables used in physical model simulations (b).

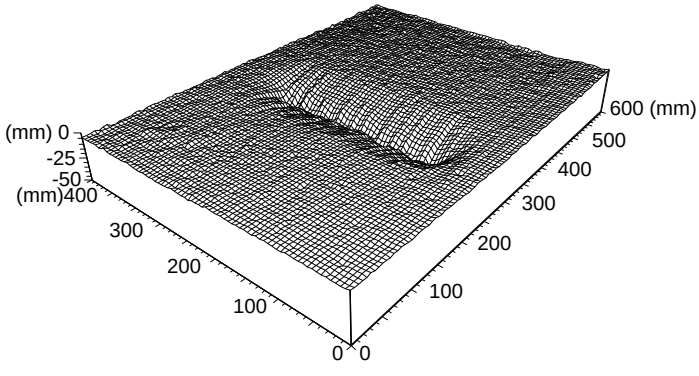

Figure 2 Example of three-dimensional laser scanned image of subsidence of sand overburden.

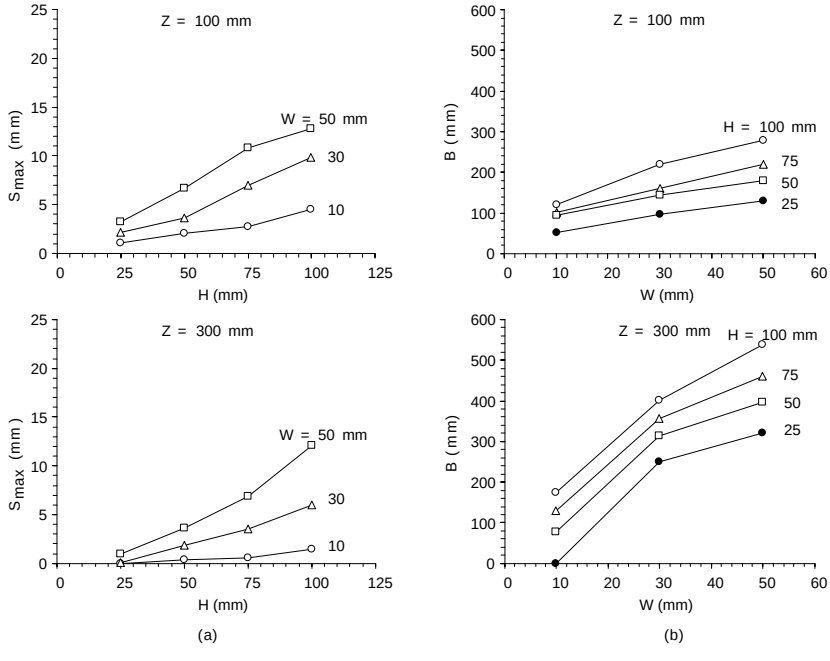

Figure 3 (a) Example of maximum subsidence (S_{max}) as a function of opening height (H), and (b) trough width (B) as a function opening width (W).

4. Numerical Simulations

Discrete element analyses using PFC^{2D} [21] are performed to compare the results with those of the physical models. The primary objectives are to verify the physical model results and to allow extrapolating the numerical model results to the conditions beyond those used in the physical modeling. The parameters used in the PFC^{2D} model are identical to those of the physical model tests. The properties of the sand overburden are given in section 2. The particle radius is 1 mm, friction angle = 22.7 degree, bulk density = 1,455 kN/m^3, friction coefficient = 0.46, normal stiffness (K_n) = 44.54 GPa/m, and shear stiffness (K_s) = 0.73 GPa/m. Several friction angles are assumed varying from 20, 25, 30 to 35 degrees. The cohesion is taken as zero for all cases (cohesionless material). The assumption of zero cohesion used here is also supported by the experimental results of Barton [22], Crosby [23] and Grøneng et al. [24] who found that the cohesion of rock mass comprising claystone, mudstone and siltstone is zero or negligible. The boundary conditions defined in the PFC^{2D}, are similar to those used in the physical models. After the particles are at rest and the model equilibrium at the predefined overburden thickness, the wall above the opening is deleted to simulate the solutioned cavern. No lateral pressure is applied. The particles are continuously flowed in to the opening until the opening is filled, and subsequently the surface subsidence is induced. Figure 4 compares the physical model results with the PFC^{2D} simulations for some example cases. The PFC^{2D} simulations agree well with those observed from the physical model testing.

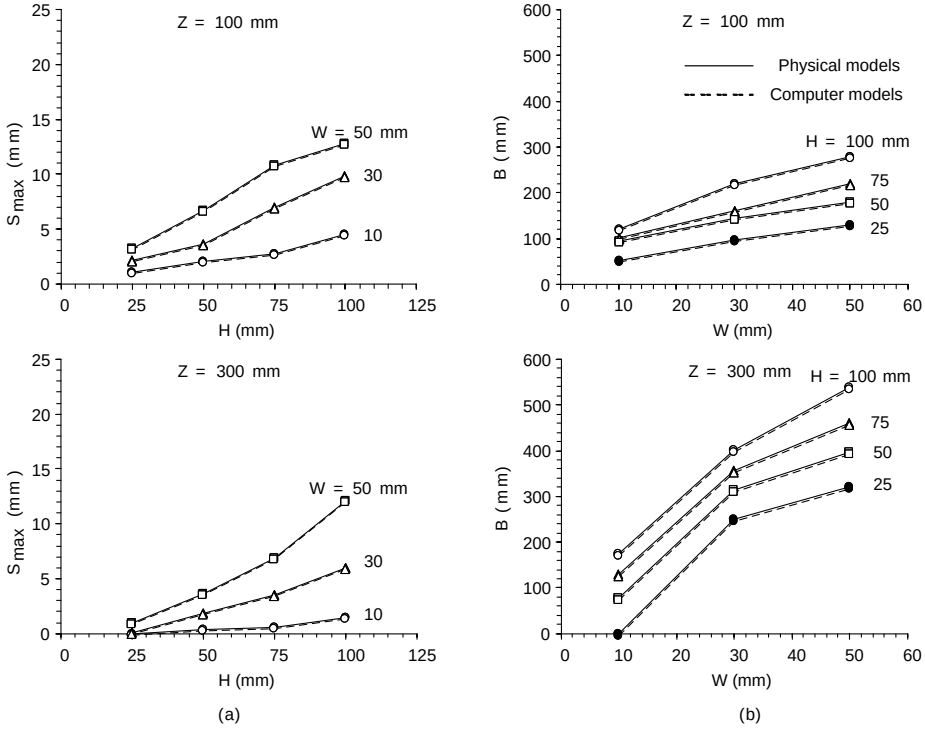

Figure 4 Comparisons between physical model results (solid lines) and PFC model simulations (dash lines) for depths of 100 and 300 mm.

5. Mathematical Relationship

An attempt is made to derive mathematical relationships between the measured subsidence components and the test variables. The opening height (H), opening width (W), maximum subsidence (S_{max}) and opening depth (Z) are first equivalented by the size of test particle (2 mm). This approach can isolate the particle size effect, and hence allows as to correlate with the modeling results actual field condition where the particle sizes of the overburden may be as larger as 5 cm. And the cavern widths and heights may exceed 10 m. Figure 5(a) plots the equivalent opening height (H_e) as a function of equivalent subsidence which is normalized by the equivalent opening depth (S_e/Z_e). Empirical equation is proposed to represent the equivalent opening height as a function of normalized subsidence, as follows:

$$H_e = A \cdot S_e/Z_e^{B} \quad (1)$$

where A and B are empirical constants. Based on linear regression analyses of the results from the physical models in Figure 5(a) it is found that the parameter A tends to be constant at 1600, and the B values can be defined as a function of equivalent trough width and opening depth, as follows:

$$B = -\alpha \cdot (B_e/Z_e) - \beta \quad (2)$$

where α and β are constants equal to 0.6 and 0.41. They probably depend on the properties of the sand overburden.

Figure 5(b) shows the equivalent opening width (W_e) as a function of equivalent maximum subsidence that is normalized by the equivalent opening depth (S_e/Z_e). Similar to the equivalent height equation (1) above an empirical equation is proposed to represent the opening width as a function of normalized subsidence obtained from the physical model results, as follows:

$$W_e = C \cdot S_e/Z_e^{D} \quad (3)$$

$$D = -\lambda \cdot \ln (B_e/Z_e) - \kappa \quad (4)$$

where C, λ and κ are empirical constants, which are equal to 2.03, 0.70 and 0.35. Again these constants would depend on the properties of the overburden.

To find the relationship between the constants above and the overburden properties, series of numerical simulations are performed using the friction angles varying from 20, 25, 30 to 35 degrees. Figure 6 compares the numerical model results with the predictions given by equations (1) and (2). The equivalent opening height (H_e) as a function of normalized maximum subsidence (S_e/Z_e) for various normalized opening widths (B_e/Z_e) obtained from the equations agree well with the computer simulations. For each width, the opening height increases with the maximum subsidence S_e/Z_e, which can be described by the power equation. It is found that the empirical constants A and B depend on the friction angles of the overburden which can be described by a linear equation:

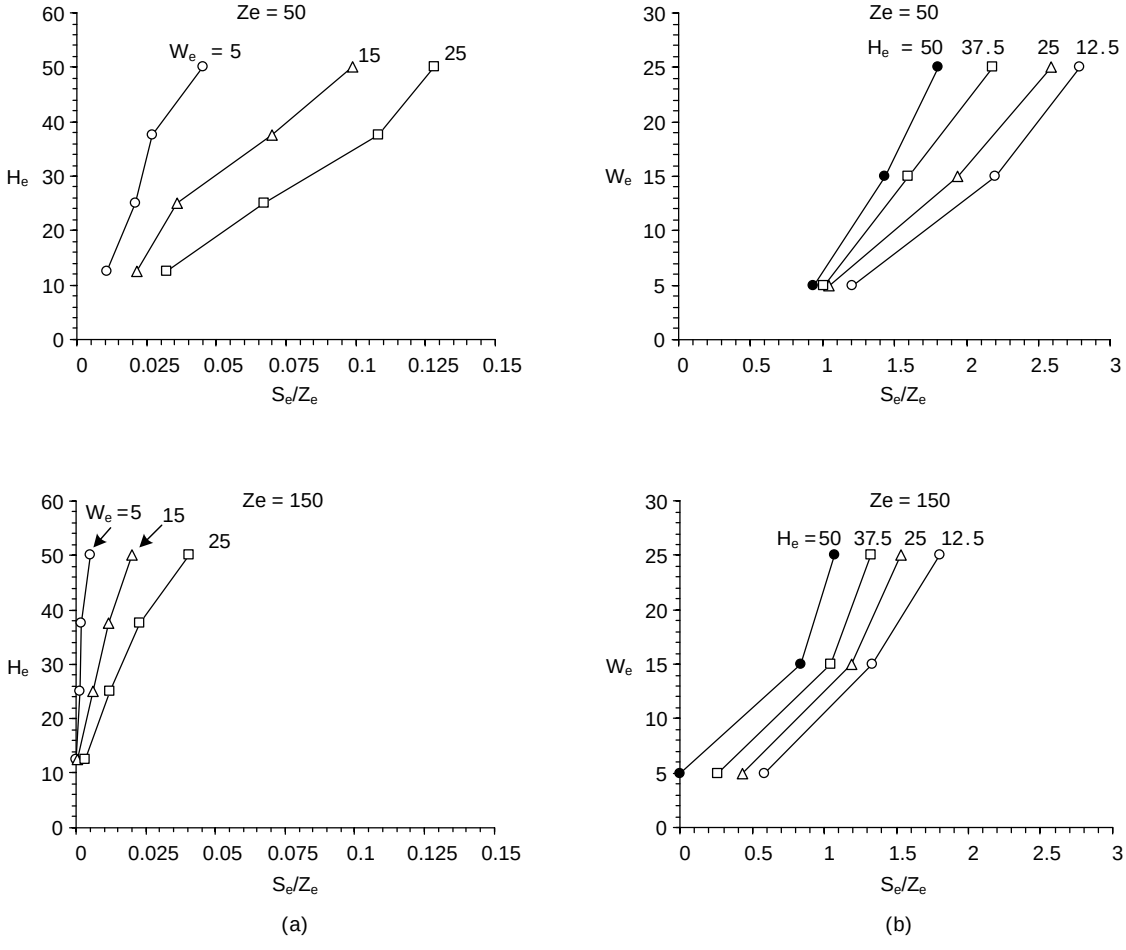

Figure 5 (a) Equivalent opening height (H_e) as a function of normalize maximum subsidence (S_e/Z_e), and (b) equivalent opening width (W_e) as a function of normalize trough width (B_e/Z_e).

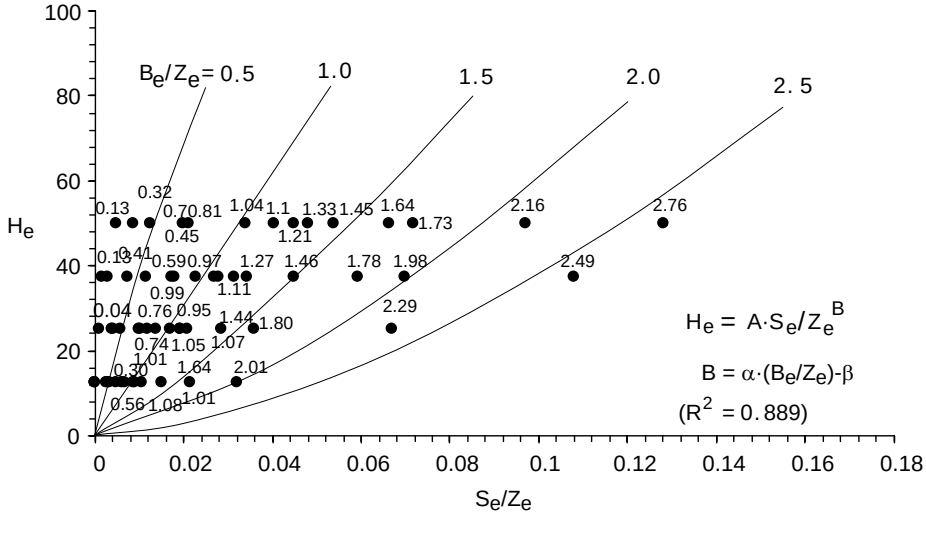

Figure 6 Curve fits for equivalent opening height (H_e) compared with the computer simulations.

$$A = -328 \cdot \phi + 11.5 \times 10^3 \quad (5)$$

$$B = -0.08 \cdot \phi + 3.02 \quad (6)$$

where ϕ used in the computer simulations are 20, 25, 30, and 35 degrees

The equivalent opening width increases with increasing normalized trough width, as shown in Figure 7. Similar to the equivalent opening height equations above, the equivalent opening width can be expressed as a function of S_e/Z_e as:

$$W_e = C \cdot S_e/Z_e^{-\lambda \cdot \ln (Be/Ze) - \kappa} \quad (7)$$

where C, λ and κ are obtained from the regression analysis equal to 2.03, 0.70 and 0.35. These parameters are independent of the friction angle of the overburden.

It should be noted that the maximum subsidence and trough width in the equations above are normalized by the equivalent opening depth. The depth of the solutioned cavities are usually known from the depth of the pumping wells used to draw the brine directly above the salt bed.

6. Discussions and Conclusions

The close agreement between the numerical simulations and the physical model measurements suggests that the procedure and results of the physical modelling are accurate and reliable (Figure 4). Both approaches indicate that the increase of the maximum subsidence closely relates to the increase of opening height, while the increase of trough widths is related to the increase of opening width. The S_{max} values tend to be independent of the opening depths or overburden thickness. The trough width however is more sensitive to the overburden thickness. This agrees with the postulation given by Singh [25] that under super-critical subsidence condition the maximum subsidence tends to be constant, while the trough width tends to increase with the opening width. Equations in Figures 6 and 7 can be used individually to estimate the opening height (H_e) and opening width (W_e). This is primarily because H_e is largely governed by S_{max}, while W_e is controlled by trough width, B, as suggested by the physical model results presented in section 3. The proposed mathematical equations may be used as a predictive tool to estimate the cavern height and width based on the subsidence trough size and shape and the friction angle of the overburden materials. Subsequently, remedial measure may be implemented to minimize the impact from the cavern development before severe subsidence or sinkhole occurs.

Acknowledgements

This study is funded by Suranaree University of Technology and by the Higher Education Promotion and National Research University of Thailand. Permission to publish this paper is gratefully acknowledged.

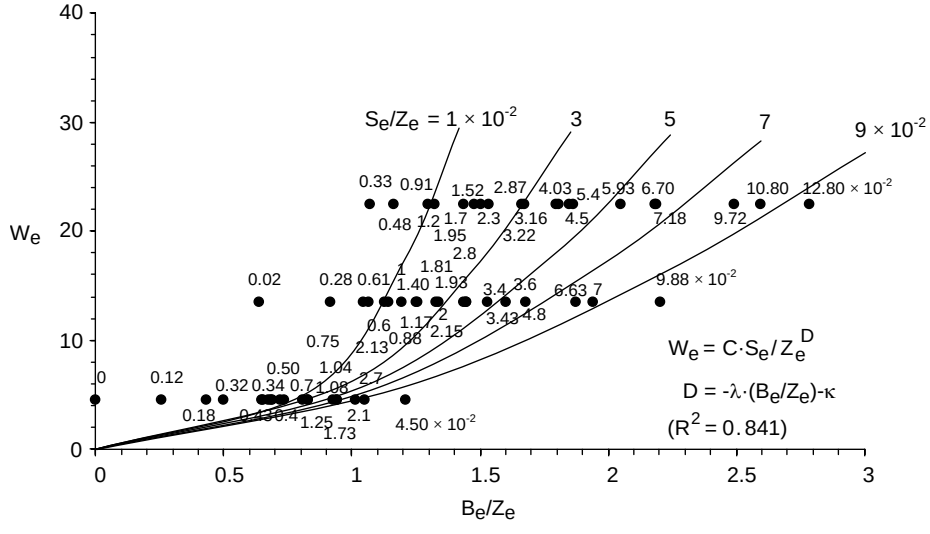

Figure 7 Curve fits for equivalent opening height (W_e) compared with the computer simulations (points).

References

[1] Fuenkajorn, K. Design guideline for salt solution mining in Thailand. *Research and Development Journal of the Engineering Institute of Thailand*, 2002, 13(1), pp. 1-8.

[2] Wannakao, L. *et al.* Geotechnical investigation of surface subsidence at Ban Non Sabaeng salt production area, Sakon Nakhon, Thailand. *International Conference on Geology, Geotechnical and Mineral Resources of Indochina (GEOINDO 2005)*, Khon Kaen University, 2005, pp. 282.

[3] Jenkunawat, P. Results of drilling to study occurrence of salt cavities and surface subsidence Ban Non Sabaeng and Ban Nong Kwang, Amphoe Ban Muang, Sakon Nakhon. *International Conference on Geology, Geotechnical and Mineral Resources of Indochina (GEOINDO 2005)*, Khon Kaen University, 2005, pp. 259-267.

[4] Jenkunawat, P. Results of drilling to study occurrence of salt cavities and surface subsidence Ban Non Sabaeng and Ban Nong Kwang, Sakon Nakhon. *Proceedings of the First Thailand Symposium on Rock Mechanics*, Suranaree University of Technology, 2007, pp. 257-274.

[5] Liu, Y. *et al.* An experimental and numerical investigation on the deformation of overlying coal seams above double-seam extraction for controlling coal mine methane emissions. *International Journal of Coal Geology,* 2001, 187, pp. 139 – 149.

[6] Fuenkajorn, K. and Archeeploha, S. Estimation of cavern configurations from subsidence data. *Bulletin of Engineering Geology and the Environment*, 2011, 70, pp. 53-61.

[7] Helm, P. R. *et al*. Numerical modelling of shallow abandoned mine working subsidence affecting transport infrastructure. *Engineering Geology*, 2013, 154, pp. 6-19.

[8] Li, Z. and Wang, J. Accident investigation of mine subsidence with application of particle flow code. *Procedia Engineering*, 2011, 26, 1698-1704.

[9] Lisjak, A. and Grasselli, G. A review of discrete modelling techniques for fracturing process in discontinuous rock masses. *Journal of Rock Mechanics and Geotechnical Engineering*, 2004, 6, pp. 301-314.

[10] Terzaghi, K. Stress distribution in dry and in saturated sand above a yielding trap-door. *Proceedings of the International Conference on Soil Mechanics*, Cambridge, 1936, pp. 307-311.

[11] Adachi, T. *et al.* Experimental study on the distribution of earth pressure and surface settlement through three-dimensional trapdoor tests. *Tunnelling and Underground Space Technology*, 2003, 18, pp. 171-183.

[12] Ghabraie, B. *et al.* Physical modelling of subsidence from sequential extraction of partially overlapping longwall panels and study of substrata movement characteristics. *International Journal of Coal Geology*, 2015, 140, pp. 71-83.

[13] Park, S. H. *et al.* Trap door test using aluminum blocks. *Proc. of the 29th U.S. Symposium of Rock Mechanics*, 1999, 106-111.

[14] Meguid, M. A. *et al.* Physical modeling of tunnels in soft ground: A review. *Tunnelling and Underground Space Technology*, 2008, 23, pp. 185-198.

[15] ASTM Standard D422-63, Standard Test Method for Particle-Size Analysis of Soils. *Annual Book of ASTM Standards, American Society for Testing and Materials*, West Conshohocken, PA, 2007.

[16] ASTM Standard D2487-06, Standard Practice for Classification of Soils for Engineering Purposes (Unified Soil Classification System). *Annual Book of ASTM Standards, American Society for Testing and Materials*, West Conshohocken, PA, 2006.

[17] Power, M. C. A new roundness scale for sedimentary particle. *Journal of Sedimentary Research,* 1953, pp. 117-119.

[18] ASTM Standard D5607-08, Standard Test Method for Performing Laboratory Direct Shear Strength Tests of Rock Specimens Under Constant Normal Force. *Annual Book of ASTM Standards, American Society for Testing and Materials*, West Conshohocken, PA, 2008.

[19] Thongprapha, T. *et al.* Study of surface subsidence above an underground opening using a trap door apparatus. *Tunnelling and Underground Space Technology*, 2015, 46, pp. 94-103.

[20] Saoanunt, N. and Fuenkajorn, K. Physical model simulations of super-critical subsidence as affected by mining sequence and excavation rate. *In 9th South East Asia Technical University Consortium (SEATUC) Symposium*, Suranaree University of Technology, 2015, pp. 22-25.

[21] Itasca. *User Manual for Particle Flow Code in 2 Dimensions*, Version 4.0, Itasca Consulting Group Inc., Minnespolis: MN, 2008.

[22] Crosby, K. Integration of rock mechanics and geology when designing the Udon South sylvinite mine. *Proceedings of the First Thailand Symposium on Rock Mechanics*, Suranaree University of Technology, 2007, pp. 3-22.

[23] Barton, N. R. A review of the shear strength of filled discontinuities in rock. *Norwegian Geotechnology Institute of Oslo*, 1974, pp. 105.

[24] Grøneng, G. *et al.* Shear strength estimation for Åknes sliding area in western Norway. *International Journal of Rock Mechanics and Mining Sciences*, 2009, 46 (3), pp. 479-488.

[25] Singh, M. M. *SME Mining Engineering Handbook*, Society for Mining Metallurgy and Exploration: Colorado, 1992.